

## 8 SCIENTIFIC HIGHLIGHT OF THE MONTH: "Optical Properties of Correlated Materials – or Why Intelligent Windows may look Dirty"

---

### Optical Properties of Correlated Materials – or Why Intelligent Windows may look Dirty

Jan M. Tomczak<sup>1,3</sup>, Silke Biermann<sup>2,3</sup>

<sup>1</sup>Research Institute for Computational Sciences, AIST, Tsukuba, 305-8568 Japan

<sup>2</sup>Centre de Physique Théorique, Ecole Polytechnique, CNRS,  
91128 Palaiseau Cedex, France

<sup>3</sup>Japan Science and Technology Agency, CREST

#### Abstract

Materials with strong electronic Coulomb correlations play an increasing role in modern materials applications. "Thermochromic" systems, which exhibit thermally induced changes in their optical response, provide a particularly interesting case. The optical switching associated with the metal-insulator transition of vanadium dioxide ( $\text{VO}_2$ ), for example, has been proposed for use in numerous applications, ranging from anti-laser shields to "intelligent" windows, which selectively filter radiative heat in hot weather conditions.

Are present-day electronic structure techniques able to describe, or – eventually even predict – such a kind of behavior? How far are we from materials design using *correlated oxides*? These are the central questions we try to address in this Highlight.

We review recent attempts of calculating optical properties of correlated materials within dynamical mean field theory, and present results for vanadium dioxide obtained within a novel scheme aiming at particularly simple and efficient calculations of optical matrix elements within localized basis sets.

Finally, by optimizing the geometry of "intelligent windows", we demonstrate that this kind of technique can in principle be used to provide guidance for experiments, thus giving a rather optimistic answer to the above questions.

## 1 Towards Materials Design for Correlated Materials ?

August is the month when (at least in southern European countries) air-conditioning bills are peaking. The reader will thus forgive us if we start the August  $\Psi_k$  Scientific Highlight by describing a proposal made by materials scientists geared at saving air-conditioning costs [1–3].

As a function of temperature, vanadium dioxide ( $\text{VO}_2$ ) undergoes a metal-insulator transition [4]. The changes through this transition are such that, coating your window with a thin layer of  $\text{VO}_2$

may – under certain conditions (see below) – create a fenestration that is “intelligent” in the following sense : At low temperatures, when  $\text{VO}_2$  is in its insulating regime, the transmission properties change only remotely with respect to the bare glass window, whereas infrared radiation is filtered when the oxide layer switches to its metallic phase in hot weather conditions. Then, heat radiation is substantially prevented from entering the building and there is less need for energy-intensive cooling by air-conditioning.

In geographical regions, where seasonal temperature changes are important (and this encompasses in particular the industrialized world), these “thermochromic” windows are clearly superior to “static” window coatings [5], that filter certain wavelengths irrespective of external conditions and which thus would increase the need for heating buildings during winter.

Even if in vanadium dioxide the changes of its properties with temperature are particularly abrupt,  $\text{VO}_2$  is by no means the only material where a tiny change in external parameters can radically modify the physical properties. In fact, such behavior can nearly be considered a hallmark of materials with strong electronic Coulomb interactions<sup>1</sup>. The concerted behavior of electrons in correlated materials causes indeed quite in general an extreme sensitivity to external stimuli, such as temperature, pressure or external fields. Heating insulating  $\text{SmNiO}_3$  beyond 400 K or applying a pressure of just a few kbar to the Mott insulator  $(\text{V}_{1-x}\text{Cr}_x)_2\text{O}_3$  ( $x=0.01$ ) [6], for example, makes the materials undergo transitions to metallic states. This tuneability of even fundamental properties is both, a harbinger for diverse technological applications and a challenge for a theoretical description.

An increasing role is nowadays played by artificial structures, ranging from multilayers that display the giant magnetoresistance effect (widely used in storage devices) [7, 8] to functional surfaces, where appropriate coatings e.g. provide a self-cleaning mechanism [9]. The huge freedom in the design, which concerns not only parameters such as the chemical composition, the doping and the growth conditions, but also the geometry of the device (e.g. the layer thicknesses), however makes the search for devices with specific electronic properties a tedious task. This leads us to the central question of the present Highlight : Can modern first principles calculations help in the quest for promising materials and setups for particular devices? The aim can of course not be to replace experiments, but rather to provide some guidance in order to minimize expensive experimental surveys and prototypings.

The Achilles heel of electronic structure theory is the description of electronic many-body interactions. Indeed, a great majority of materials used in modern applications fall in the class of so-called “strongly correlated materials” where electron-electron interactions profoundly modify (if not invalidate) a pure band picture [6]. State-of-the-art first principles methods, such as density functional theory, are then no longer sufficient to predict the physical properties of these materials. Despite these difficulties, in this Highlight we give a quite optimistic view on the above question.

In fact, important steps to bridge the gap between band structure methods and many-body physics have been made in recent years. For materials with moderately strong correlations, Hedin’s GW approximation [10] – which has seen increasingly sophisticated implementations

---

<sup>1</sup>Vanadium dioxide could in some sense be considered an exception due to the fact that it may be less correlated than many of the other examples.

in the electronic structure context [11–14] – has established itself as a method of choice. For strongly correlated materials, progress was for instance brought about by combining density functional theory within the local density approximation [15] with dynamical mean field theory (DMFT) [16]. The resulting approach, dubbed LDA+DMFT [17,18] (for reviews see [19–21]), joins the accurate description of strong local Coulomb correlations in a many-body framework with the material-specific information provided by state-of-the-art band theory. It has – over the last years – helped to elucidate physical mechanisms at work in systems such as transition metals [22–25], their oxides [26–34] or sulphides [35,36], as well as f-electron compounds [37–40]. The number of applications is nowadays too large to give a complete list in this Highlight, but recent reviews provide an extensive picture [19–21,41].

While tremendous progress has been achieved, there remains a chasm between what state-of-the-art electronic structure methods can calculate and what experimentalists are actually measuring. On the one hand, the chemical complexity of many systems does simply not (yet) allow for being tackled by costly many-body techniques. On the other hand, the variety of experimental observables that are being computed for the sake of comparison is rather unsatisfactory. It is therefore an important task to make more experimentally measurable quantities accessible from theoretical calculations.

Within dynamical mean field theory, emphasis is commonly put on *spectral* properties, and the evaluation of observables other than spectral functions is a rather new advancement in the realistic context. Yet, it is rather the *response* behavior of correlated materials that is promising for applications.

In this Highlight, we review some recent attempts of calculating optical properties of correlated materials, and explore the implications for technological applications on the specific example of VO<sub>2</sub>-based intelligent windows.

## 2 Optical Spectroscopy

### 2.1 General formula and some physical implications

Numerous experimental techniques have been devised for and applied to the study of correlated materials of ever growing complexity. Optical spectroscopy, which is the subject of this work, is, in a way, the most natural among them : Optical detectors are sampling the response to incident light, as do our eyes, albeit accessing frequencies, and thus phenomena, that are beyond our vision. The technique is particularly suited to track the evolution of a system under changes of external parameters like temperature or pressure. This is owing to a generally high precision, and the fact that, contrary to e.g. photoemission spectroscopy or x-ray experiments, results are obtained in absolute values. Especially, the existence of sum-rules (see e.g. [42,43]) allows for a quantitative assessment of transfers of spectral weight upon the progression of the system properties. Moreover, while in photoemission the electron escape depth and thus surface effects are often an issue, the larger skin penetration depth assures that optical spectroscopy is a true bulk probe. One might add that the transition matrix elements are also better understood in optics (this is an important part in this work) than in photoemission (see e.g. [44]). On the other

hand, response functions are two-particle quantities that are less obvious in their interpretation than a one-particle spectrum. An important simplification is achieved when neglecting vertex corrections. In the framework of linear response theory, the optical conductivity can then be expressed as (for reviews see [34, 42])

$$Re \sigma^{\alpha\beta}(\omega) = \frac{2\pi e^2 \hbar}{V} \sum_{\mathbf{k}} \int d\omega' \frac{f(\omega') - f(\omega' + \omega)}{\omega} \text{tr} \left\{ A_{\mathbf{k}}(\omega' + \omega) v_{\mathbf{k},\alpha} A_{\mathbf{k}}(\omega') v_{\mathbf{k},\beta} \right\} \quad (1)$$

Here,  $A_{\mathbf{k}}(\omega)$  is the momentum-resolved many-body spectral function, and different optical transitions are weighted by the Fermi velocities  $v_{\mathbf{k},\alpha} = \frac{1}{m} \langle \mathbf{k}L' | \mathcal{P}_{\alpha} | \mathbf{k}L \rangle$ , matrix elements of the momentum operator  $\mathcal{P}$ . Both, spectral functions and velocities are matrices in orbital space  $L$ , which we will specify later on. The Fermi functions  $f(\omega)$  select the range of occupied and empty energies, respectively,  $V$  is the unit-cell volume,  $\alpha, \beta$  denote cartesian coordinates, and  $Re \sigma^{\alpha\beta}$  is the response in  $\alpha$ -direction for a light polarization  $E$  along  $\beta$ .

To get an idea about the physical content of this formula, we first consider some archetypical cases. At zero temperature, and for a system that is well described by its band structure as given by density-functional theory (DFT) based methods, the (Kohn-Sham) spectrum is the defining quantity, since vertex corrections are absent<sup>2</sup>. Moreover, the spectral functions  $A(\mathbf{k}, \omega)$  of the system become Dirac distributions and the trace in Eq. (1) reads<sup>3</sup>

$$\sum_{m,n} \delta(\omega' + \omega + \mu - \epsilon_{\mathbf{k}}^m) v_{\mathbf{k}}^{mn} \delta(\omega' + \mu - \epsilon_{\mathbf{k}}^n) v_{\mathbf{k}}^{nm} \quad (2)$$

While at finite frequencies,  $\omega > 0$ , only inter-band transitions,  $m \neq n$ , can give a contribution, we see that at zero frequency,  $\omega = 0$ , and provided a band  $\epsilon_{\mathbf{k}}^n$  is crossing the Fermi level, the response is a delta function deriving from intra-band transitions<sup>4</sup>. The latter is just the result of the fact that without interactions (electron-electron correlations or a coupling to a bosonic mode) or disorder, the lattice momentum  $\mathbf{k}$  is a constant of motion and the current thus does not decay.

In the (effective) non-interacting case the response of a metal to an electric field is thus infinite. It was P. Drude in 1900 who derived an expression that takes into account the finite lifetime of the electron excitations, by introducing a relaxation time  $\tau$  for the charge current  $j(t) = j(0)e^{-t/\tau}$ . His expression for the conductivity can be recovered from our linear response result, Eq. (1), by assuming free particles,  $\epsilon_{\mathbf{k}} = \frac{\hbar^2 k^2}{2m}$ , and a constant self-energy  $\Sigma = -\frac{\hbar}{2\tau}$ . The resulting optical conductivity is then given by

$$Re \sigma(\omega) = \frac{ne}{m} \frac{\tau}{1 + \omega^2 \tau^2} \quad (3)$$

with  $n$  being the average charge carrier density. Hence, the response at zero frequency is finite and non-zero at finite energies.

---

<sup>2</sup>There are thus two effects that DFT does not account for : (a) In general, it lacks the correct spectrum. This is mended by the formalism described above, since it uses spectral functions stemming from a many-body calculation. (b) The particle-hole interaction (vertex corrections). This is not addressed in the above formalism and remains a challenge for future work. We note that vertex corrections vanish within DMFT (infinite dimensions) in the one-band case [45]. For the current multi-orbital case, this is however an approximation. Within GW [11], vertex corrections are included on the RPA level. However, GW *spectra* may not be sufficient for strongly correlated systems.

<sup>3</sup>for simplicity we assume to work in the Kohn-Sham basis, i.e. the spectral function  $A_{\mathbf{k}}(\omega)$  is diagonal.

<sup>4</sup>or transitions within degenerate bands,  $\epsilon_{\mathbf{k}}^n = \epsilon_{\mathbf{k}}^m$ , while  $m \neq n$ .

While the physical picture about the origin of the relaxation time had to be revised with the advent of quantum mechanics and Bloch’s theory of electronic states in periodic potentials, Drude’s theory still accounts well for the response of simple metals. However, it becomes insufficient, even in the one-band case, in the presence of substantial correlation effects. Indeed, the influence of electronic interactions is beyond a mere broadening of bands. For the case of the one-band Hubbard model within DMFT, the paramount characteristic is the appearance of Hubbard satellites in the spectral function. Therewith, not only transitions within a broadened quasi-particle peak are possible (à la Drude), but also transitions from and to these Hubbard bands arise [46, 47]. Thus, in such a metal two additional contributions occur, stemming from transitions between the quasi-particle peak and the individual Hubbard bands. This feature is often referred to as the mid-infrared peak, due to its location in energy in some compounds. At higher energy, transitions between the two Hubbard bands appear. In the Mott insulating phase, only the latter survive. Therewith the complexity of optical spectra is considerably enhanced [46, 47] with respect to the independent particle picture.

Within DMFT, calculations of the optical conductivity were first performed by Pruschke and Jarrell *et al.* [48, 49] for the case of the Hubbard model. Rozenberg *et al.* [46, 47] studied the phenomenology of the different optical responses of the Hubbard model throughout its phase diagram, discussing the above described phenomenology and comparing it to experiments on  $V_2O_3$ . With the advent of LDA+DMFT, optical conductivity calculations gained in realism: Blümer *et al.* [50, 51] and later on Pavarini *et al.* [52] and Baldassarre *et al.* [53] used the LDA+DMFT spectral functions for the calculation of titanate and vanadate optical spectra. A more general approach, was developed by Pálsson [54] for the study of thermo-electricity. Our work [34, 55–57] goes along the lines of these approaches. We will however employ a formulation using the full valence Hamiltonian therewith allowing for the general case including interband transitions and we extend the intervening Fermi velocities to multi-atomic unit cells, which becomes crucial in calculations for realistic compounds.

Alternative techniques were proposed by Perlov *et al.* [58, 59] and by Oudovenko *et al.* [60]. The former explicitly calculated the matrix elements, albeit using a different basis representation than in the DMFT part, while the latter diagonalized the interacting system, which allows for the analytical performing of some occurring integrals due to the “non-interacting” form of the Green’s function. Owing to the frequency-dependence of the self-energy, however, the diagonalization has to be performed for each momentum and frequency separately so that the procedure may become numerically expensive. This technique has in particular been applied to elucidate the  $\alpha - \gamma$  transition in Ce [61], and, more recently, to the heavy fermion compound  $CeIrIn_5$  [62].

The calculation of accurate absolute values of the optical response has however turned out to be a challenge which mainly stems from the way the Fermi velocities are treated. In view of predictive materials design accurate absolute values in the optical conductivity are a condition *sine qua non*.

## 2.2 A scheme for the optical conductivity using localized basis sets

Correlation effects enter the calculation of the optical conductivity, Eq. (1), only via the spectral functions  $A_{\mathbf{k}}(\omega)$ , while the Fermi velocities  $v_{\mathbf{k},\alpha} = \frac{1}{m} \langle \mathbf{k}L' | \mathcal{P}_\alpha | \mathbf{k}L \rangle$  are determined by the one-particle part of the system<sup>5</sup>.

While the computation of the latter is straightforward in a plane-wave setup, the application of many-body techniques such as LDA+DMFT, necessitates the use of localized basis sets (see e.g. [63]). It is thus convenient to express also the Fermi velocities in terms of this basis. Therewith, however, the evaluation of matrix elements of the momentum operator (see above) becomes rather tedious. The aim of the current approach is to employ a controlled approximation to the full dipole matrix elements in a Wannier like basis set that is accurate enough to yield absolute values of the conductivity to allow for a quantitative comparison with experiment.

We choose our orbital space by specifying  $L = (n, l, m, \gamma)$ , with the usual quantum numbers  $(n, l, m)$ , while  $\gamma$  denotes the atoms in the unit cell :  $|\mathbf{k}L\rangle$  then is the Fourier transform of the Wannier function  $\chi_{\mathbf{R}L}(\mathbf{r})$  localized at atom  $\gamma$  in the unit cell  $\mathbf{R}$ . Extending the well-known Peierls substitution approach for lattice models (see the review [42]) to the realistic case of multi-atomic unit cells, we find that

$$v_{\mathbf{k},\alpha}^{L'L} = \frac{1}{\hbar} \left( \partial_{k_\alpha} \mathbf{H}_{\mathbf{k}}^{L'L} - i(\rho_{L'}^\alpha - \rho_L^\alpha) \mathbf{H}_{\mathbf{k}}^{L'L} \right) + \mathcal{F}_{\mathbf{H}} \left[ \{ \chi_{\mathbf{R}L} \} \right] \quad (4)$$

Here,  $\rho_L$  denotes the position of an individual atom within the unit-cell. The term in brackets, which is used in the actual calculations, is in the following referred to as the “generalized Peierls” term : While the derivative term is the common Fermi velocity, the term proportional to the Hamiltonian originates from the generalization to realistic multi-atomic unit-cells and accounts for the fact that while the periodicity of the lattice is determined by the unit-cell, the Peierls phases couple to the real-space positions of the individual atoms. The correction term that recovers the full matrix element is denoted  $\mathcal{F}$  (for its explicit form see [34]). The latter reduces to purely atomic transitions,  $(\mathbf{R}, \gamma) = (\mathbf{R}', \gamma')$ , in the limit of strongly localized orbitals. In other words, the accuracy of the approach is controlled by the localization of the basis functions. This generalized Peierls approach has in particular been shown to yield a good approximation for systems with localized orbitals, such as the 3d or 4f orbitals in transition metal or lanthanide/actinide compounds [34].

## 3 Application :

### From Bulk Vanadium Dioxide to Intelligent Windows

#### 3.1 A brief reminder about the electronic structure of VO<sub>2</sub>

The electronic structure of VO<sub>2</sub> and its metal-insulator transition has been the subject of numerous theoretical studies. We give here only a brief list of prior work, for reviews see [34, 64].

---

<sup>5</sup>While for lattice models this is only true for local density-density interactions, in the continuum formulation of a solid this requires the interaction only to be local and of two-body kind. Then the interaction part of the Hamiltonian  $\mathbf{H} = \mathbf{H}_0 + \mathbf{H}_{int}$  commutes with the position operator  $\mathcal{R}_\alpha$  and thus  $\mathcal{P}_\alpha = -im/\hbar [\mathcal{R}_\alpha, \mathbf{H}_0]$ . For details see [34].

In particular, we here do not enter at all in the decade-long discussion on whether the metal-insulator transition in  $\text{VO}_2$  should be considered as a Peierls- or a Mott transition. Our point of view on this question is summarized in [33].

While capturing structural properties surprisingly well [65], band-structure methods do not reproduce experimental spectra: in the metal, incoherent weight at higher binding energies is absent, and in the insulator the gap is not opened in the corresponding Kohn-Sham spectra. Nevertheless, thorough LDA studies [64, 65] gave useful indications and paved the road to the application of more sophisticated many-body approaches.

LDA+DMFT results for the spectral properties of  $\text{VO}_2$  agree well with experimental findings in both, the metallic [32, 66, 67] and the insulating phase [32], as can be seen from Fig. 1 which compares photoemission and LDA+DMFT spectra.

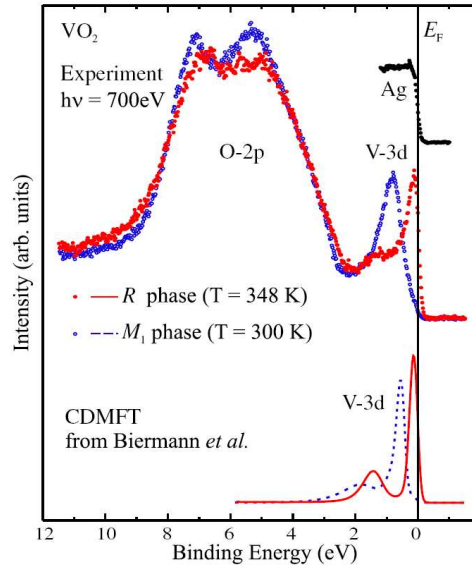


Figure 1: Comparison of valence band photoemission spectra of Koethe *et al.* [68] (top) and LDA+DMFT results from [32] (bottom). Picture from [68].

Since at least the insulating phase of  $\text{VO}_2$  is in fact relatively band-like [33], an interesting alternative approach is provided by the GW approximation [11]. While pioneering early work [69] had to resort to a simplified scheme, recently it became possible to perform fully *ab initio* GW calculations for  $\text{VO}_2$  [34, 70, 71]. Full GW calculations for the optical conductivity and the spectral function thus seem to come into reach, opening the way to systematic comparisons with DMFT results.

Our calculation of optical properties [34, 55] is footing on the LDA+DMFT electronic structure of Ref. [32] and our recent extension thereof [33, 72]. Since this many-body calculation used a downfolded Hamiltonian, we use an unfolding scheme to include optical transition from, to and between higher energy orbitals (For details see [57]).

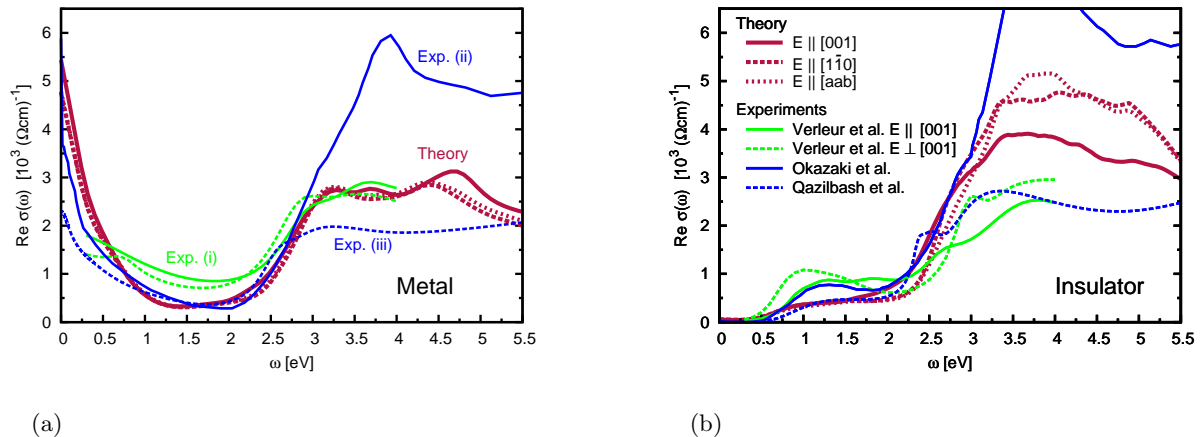


Figure 2: Optical conductivity of (a) metallic, (b) insulating  $\text{VO}_2$  for polarizations  $E$ . Theory (red) ( $[aab]=[0.85 \ 0.85 \ 0.53]$ ), experimental data (i) single crystals [73] (green), (ii) thin film [75] (solid blue), (iii) polycrystalline film [74] (dashed blue).

### 3.2 The bulk conductivity

In Fig. 2(a) we display the LDA+DMFT theoretical optical conductivity of the high temperature phase of  $\text{VO}_2$  as a function of frequency and in comparison with several experimental data [73–75], see also [76]. As can be inferred from the crystal structure [64], the optical response depends only weakly on the polarization of the incident light. The Drude-like metallic response (see also above) is caused by transitions between narrow vanadium 3d orbitals near the Fermi level. As a consequence, it only influences the low infra-red regime – a crucial observation as we shall see in the following. The shoulder at 1.75 eV yet stems from intra-vanadium 3d contributions, while transitions involving oxygen 2p orbitals set in at 2 eV, and henceforth constitute the major spectral weight up to the highest energies of the calculation.

In Fig. 2(b) we show the conductivity for insulating  $\text{VO}_2$ . As was the case before, the theoretical results are in good agreement with the different experiments. This time, a slight polarization dependence is seen in both, experiment and theory, owing to the change in crystal symmetry. Indeed, vanadium atoms pair up in the insulator to form dimers along the  $c$ -axis, leading to the formation of bonding/anti-bonding states for 3d orbitals<sup>6</sup> [77]. Optical transitions between these orbitals result in an amplitude of the conductivity that, in the corresponding energy range ( $\omega = 1.5 - 2.5$  eV), is higher for a light polarization parallel to the  $c$ -axis than for other directions (For a detailed discussion see [34, 56]).

<sup>6</sup>We stress that the bonding/anti-bonding splitting is not sufficient to open a gap within band-structure approaches. Indeed correlations enhance this splitting (after having transferred the  $e_g^\pi$  charge into the  $a_{1g}$  band), and we refer to this scenario as a “many-body Peierls insulator” [33].



### 3.3 Intelligent windows

Having established the theoretical optical response of *bulk* VO<sub>2</sub>, and thus verified that our scheme can *quantitatively* reproduce optical properties of correlated materials, we now investigate the possibilities of VO<sub>2</sub>-based intelligent window coatings [2, 3, 78, 79]. The effect to be exploited here can already be seen in the above responses of the bulk : The respective conductivities of both phases (Fig. 2(a), (b)) exhibit a close similarity in the range of visible light ( $\omega = 1.7 - 3.0$  eV), whereas in the infra-red regime ( $\omega < 1.7$  eV) a pronounced switching occurs across the metal-insulator transition. As a result, heat radiation will be let through at low external temperatures, while its transmission will be hindered above the transition, which reduces the need for air conditioning in e.g. office buildings. The insensitivity to temperature for visible light, in conjunction with the selectivity of the response to infrared radiation, is an essential feature of an intelligent window setup. Yet, for an applicable realization, other important requirements have to be met. First of all, the switching of the window has to occur at a relevant, i.e. ambient, temperature. Also, the total transmittance of VO<sub>2</sub>-films needs improvement in the visible range [2, 3], and the visible transmission should be rather independent of the wavelength such as to provide a colorless vision. Experimentalists have addressed these issues and have proposed potential solutions [80] : Diverse dopings,  $M_xV_{1-x}O_2$ , were proven to influence the transition temperature, with Tungsten ( $M = W$ ) being the most efficient : A doping of only 6% resulted in  $T_c \approx 20^\circ\text{C}$  [81]. However, this causes a deterioration of the infrared switching. Fluorine doping, on the other hand, improves on the switching properties, while also reducing  $T_c$  [82, 83]. An increase in the overall visible transmittance can also be achieved without modifying the intrinsic properties of the material itself, but by adding antireflexion coatings with for example TiO<sub>2</sub> [84].

Here, we address the optical properties of window coatings from the theoretical perspective. In doing so, we assume that the specular response of VO<sub>2</sub>-layers is sufficiently well-described by the optical properties of the bulk, and we use geometrical optics to deduce the properties of layered structures, as shown e.g. in Fig. 3(a), Fig. 4(a). We employ a technique equivalent to the transfer matrix method (see e.g. [85]), which accounts for the multiple reflexions within the layers. The reflectivity of the setup is then given by a recursion formula. Defining for the  $j^{\text{th}}$  layer the phase factors  $\alpha_j(\omega) = \exp(i\omega/cn_j\delta_j)$ , with  $\delta_j$  and  $n_j(\omega)$  being the layer thickness and the complex refractive index, respectively, and denoting the “bare” reflection and transmission coefficients of an isolated interface between semi-infinite layers  $j - 1, j$  by  $r_{j-1,j}, t_{j-1,j}$  one obtains a recursion formula for the “dressed” quantities  $\tilde{r}_{0,j}, \tilde{t}_{0,j}$  that account for the resulting properties of the stack of the layers  $0, 1, \dots, j$  :

$$\tilde{r}_{0,j} = \tilde{r}_{0,j-1} + \tilde{t}_{0,j-1}\tilde{t}_{j-1,0}\frac{r_{j-1,j}\tilde{\alpha}_{j-1}^2}{1 - r_{j-1,j}\tilde{r}_{j-1,0}\tilde{\alpha}_{j-1}^2} \quad (5)$$

$$\tilde{r}_{j,0} = r_{j,j-1} + t_{j,j-1}t_{j-1,j}\frac{r_{j-1,0}\tilde{\alpha}_{j-1}^2}{1 - r_{j-1,j}\tilde{r}_{j-1,0}\tilde{\alpha}_{j-1}^2} \quad (6)$$

where  $\tilde{\alpha}_j = \prod_{k \leq j} \alpha_k$  is an effective phase,  $\tilde{t}_{j,k} = 1 - \tilde{r}_{j,k}$  the complex transmission, and  $\tilde{r}_{j,0}$  the dressed reflectivity for light that reaches the setup from the opposite side.

### 3.3.1 A VO<sub>2</sub>-coated window

First, we consider the most simple possible setup, which consists of a single VO<sub>2</sub>-layer (of thickness  $d_{\text{VO}_2}$ ) on a glass substrate<sup>7</sup>. Such a window has been experimentally investigated by Tazawa *et al.* [86] and Jin *et al.* [84]. In Fig. 3 we show their measured reflectivity data as a function of wavelength, in comparison with our theoretical results.

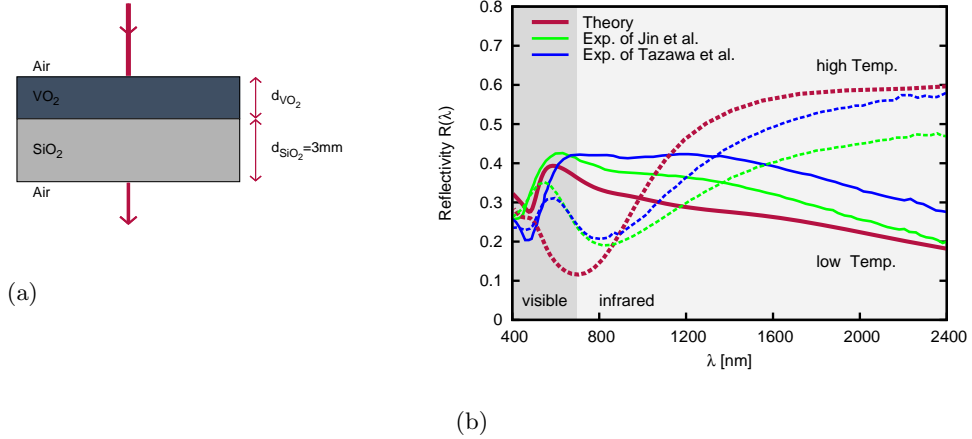


Figure 3: Setup of an intelligent window. (a) geometry of the setup : VO<sub>2</sub> on SiO<sub>2</sub>. (b) Reflectivity at high (dashed) and low temperatures (solid). Theory (red) : 60 nm VO<sub>2</sub> on SiO<sub>2</sub>. Experiments : 50 nm VO<sub>2</sub> on SiO<sub>2</sub> [84] (green), 50 nm VO<sub>2</sub> on Pyrex glass [86] (blue). All theoretical data for  $E \parallel [1\bar{1}0]$  polarization, and a 3mm SiO<sub>2</sub> substrate.

At low temperatures, i.e. insulating VO<sub>2</sub>, the calculated reflectivity is in quantitative agreement with the experimental data. In the visible range ( $\lambda \approx 400 - 700$  nm), the reflectivity depends strongly on the wavelength. Therefore, the current window will filter certain wavelengths more than others, resulting in an illumination of a certain color – an obvious drawback. Moreover, the reflectivity in this region is rather elevated, causing poor global transmission. In the infrared regime ( $\lambda > 700$  nm) – and beyond – the reflectivity decreases, and heat radiation can pass through the setup. At high temperatures, the infrared reflectivity switches to a rather elevated value, thus filtering heat radiation. The changes in the visible region are less pronounced, but still perceptible, and both, the degree of transparency and the color change through the transition. As a result, though presenting qualitative features of an intelligent window, the current setup is not yet suited for applications.

### 3.3.2 Improving the window with an anti-reflexion layer

Having established the accuracy of our approach also for the case of layered structures, we now investigate a more complicated setup. As depicted in Fig. 4(a), an additional (rutile type) TiO<sub>2</sub>-coating is added on the VO<sub>2</sub>-layer, with the objective of serving as an antireflexion filter [84]. With the thicknesses  $d_{\text{VO}_2}$  and  $d_{\text{TiO}_2}$ , the geometry of the current setup thus has already two

<sup>7</sup>We suppose quartz glass, SiO<sub>2</sub>. All auxiliary refractive indices (other than the one of VO<sub>2</sub>) are taken from *Handbook of Optical Constants of Solids* by Edward D. Palik, Academic Press, 1985.

parameters that can be used to optimize the desired optical properties. Since, however, each variation of them requires the production of a new individual sample under comparable deposition conditions, along with a careful structural characterization in order to guarantee that differences in the optical behavior are genuine and not related to variations of the sample quality, the experimental expenditure is tremendous. This led Jin *et al.* [84] to first estimate a highly transmitting setup by using tabulated refractive indices and to produce and measure only *one* such sample. Here, we shall use our theoretical results on VO<sub>2</sub> to not only optimize the geometry ( $d_{\text{TiO}_2}$ ,  $d_{\text{VO}_2}$ ) with respect to the total visible transmittance, but we shall be concerned with yet another important property of the window that needs to be controlled : its color.

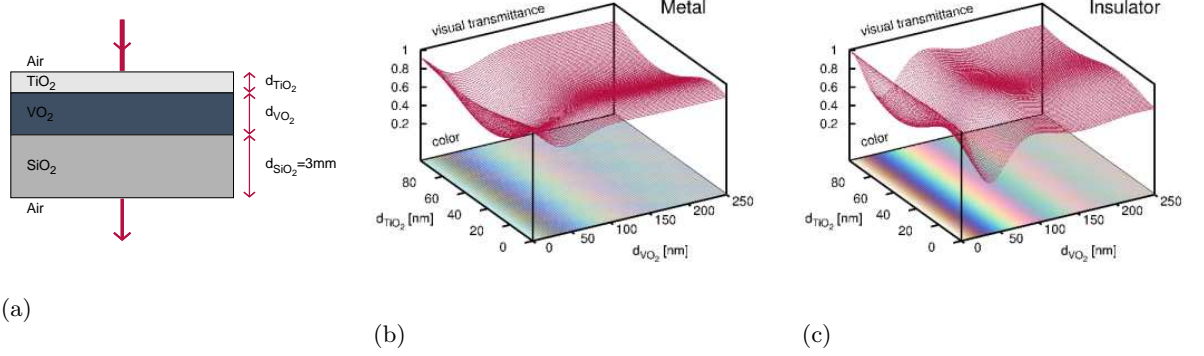


Figure 4: Setup of an intelligent window. (a) geometry of the setup : TiO<sub>2</sub> on VO<sub>2</sub> on SiO<sub>2</sub>. (b), (c) Setup with antireflexion coating : TiO<sub>2</sub> / VO<sub>2</sub> on SiO<sub>2</sub>. Shown is the normalized visible transmittance (see text) and the corresponding color of the transmitted light for (b) high and (c) low temperature as a function of the layer thicknesses  $d_{\text{VO}_2}$  and  $d_{\text{TiO}_2}$ . All theoretical data for  $E \parallel [1\bar{1}0]$  polarization, and a 3mm SiO<sub>2</sub> substrate.

Fig. 4 displays the normalized visible specular transmittance<sup>8</sup> for our window in its high (b) and low (c) temperature state, as a function of both film thicknesses. On the same graph, we moreover show the corresponding transmission color. The evolution of the light interferences within the layers results in pronounced changes in both, the overall transmittance and the color. The coating of VO<sub>2</sub> globally degrades the transparency of the bare glass window. An increase of the TiO<sub>2</sub>-coating, on the other hand, has the potential to improve on the total transmittance. This can be understood from the mechanism of commonly used quarter-wave filters. The wavelength-dependence of the real-part of the TiO<sub>2</sub> refractive index,  $n_{\text{TiO}_2}(\lambda)$ , results in an optimal quarter-wave thickness,  $\delta_{\text{TiO}_2}(\lambda) = \lambda/(4n_{\text{TiO}_2}(\lambda))$ , which varies from blue to red light only slightly from  $\delta_{\text{TiO}_2}(\lambda) = 40$  to 60 nm. This and the fact that the imaginary part of the refractive index,  $k_{\text{TiO}_2}(\lambda)$ , is negligible for visible light also explains why the color does not change significantly with  $d_{\text{TiO}_2}$ . While, as for TiO<sub>2</sub>, the variation of the real-part of the VO<sub>2</sub> refractive index yields a rather uniform ideal thickness  $\delta_{\text{VO}_2}(\lambda)$ , its imaginary part changes significantly (by a factor of 4) within the range of visible light. As a consequence, the color is very sensitive

<sup>8</sup>  $\int_{400\text{nm}}^{700\text{nm}} d\lambda S(\lambda)T(\lambda) / \int_{400\text{nm}}^{700\text{nm}} d\lambda S(\lambda)$ , with the spectrum of the light source  $S(\lambda)$ , and the transmittance  $T = 1 - R$ ,  $R$  being the specular reflexion given by Fresnel's formulae (see e.g. [43]). We thus neglect absorption due to inhomogeneities that lead to diffuse reflexion. This is justified for our applications to windows. Also, VO<sub>2</sub> has a glossy appearance and hence a preponderant specular response.

to VO<sub>2</sub>-deposition. At higher thickness  $d_{\text{VO}_2}$ , however, this dependence becomes smaller and the color lighter, as seen in Fig. 4(b) and (c). Our theoretical transmittance profiles suggest relatively thick windows to yield good visual properties. Indeed, at low temperatures (Fig. 4(c)) the local maximum that gives the thinnest window (Fig. 4(b)) is located at  $(d_{\text{TiO}_2}, d_{\text{VO}_2}) \approx (40 \text{ nm}, 85 \text{ nm})$  within our calculation. However, this setup is still in the regime of important color oscillations. Given the uncertainties in industrial deposition techniques, it seems rather cumbersome to consistently stabilize colorless samples. From this point of view, a thicker VO<sub>2</sub>-film would be desirable. Indeed, while almost preserving the overall transmittance, a colorless window at low temperatures is realized in our calculation for  $(d_{\text{TiO}_2}, d_{\text{VO}_2}) \approx (50 \text{ nm}, 220 \text{ nm})$ , or for  $(d_{\text{TiO}_2}, d_{\text{VO}_2}) = (\geq 100 \text{ nm}, 220 \text{ nm})$ . In the high temperature state, Fig. 4(b), the transmittance is globally lower than at low temperatures. Moreover, only the  $(d_{\text{TiO}_2}, d_{\text{VO}_2}) = (\geq 100 \text{ nm}, 220 \text{ nm})$  setup exhibits a simultaneously high transmittance in *both* states of the window.

## 4 Conclusions and Perspectives

In this Highlight, we have reviewed a scheme for optical properties of correlated materials that is geared at fast and accurate calculations within localized basis sets.

As an example, we have addressed – for the first time from a theoretical perspective – the fascinating application of the seemingly simple composition of vanadium dioxide in so-called intelligent windows.

Even if, from a technical point of view, possible ways of improvement in view of a fully general optics scheme are obvious – ideally, one may want to include e.g. vertex corrections, replace the LDA+DMFT starting point by a GW+DMFT calculation [87] or calculate at least the ligand-orbital energies by many-body techniques such as GW – our simple and efficient optics scheme has proven to reach quantitative agreement with experiments, at least for materials where excitonic effects are negligible. We have shown that it is not only useful to address questions of fundamental physics, but that one can indeed think of exploiting present day techniques for applied purposes.

One may argue, of course, that a crucial ingredient entering LDA+DMFT calculations is a reliable estimate for the local Coulomb interactions, the Hubbard U. In general, it is probably a fair statement to say that – despite a number of techniques that have by now been proposed for the calculation of U (constrained LDA [88], constrained RPA [89,90], or GW+DMFT [87,91,92]) – its determination still presents one of the bottlenecks for *ab initio* materials design. The recently much discussed new family of iron pnictide superconductors provides an interesting test case for calculations of U [93,94], where we dispose of little *a priori* knowledge.

For vanadium dioxide, however, this issue seems to be more a conceptual than a practical one, since experimental and theoretical estimates finally converge towards a common answer.

In conclusion, we thus give an optimistic answer to the central question of this Highlight : electronic structure techniques can – if not design – at least help guiding the search for functional materials and their devices, and this even for the particularly challenging class of correlated

materials.

## Acknowledgements

We thank the numerous colleagues, with whom we have had fruitful discussions, collaborations and exchanges on different aspects related to this research, in particular : O.K. Andersen, F. Aryasetiawan, T. Gacoin, G. Garry, M. Gatti, A. Georges, K. Haule, H.J. Kim, G. Kotliar, A.I. Lichtenstein, M. Marsi, T. Miyake, V. Oudovenko, A.I. Poteryaev, J.P. Pouget, L. Pourovskii, M.M. Qazilbash, L. Reining, R. Sakuma, E. Wimmer, R. Windiks.

This work was supported by the French ANR under project CORRELMAT, and a computing grant by IDRIS Orsay under project number 081393.

## References

- [1] Charles B. Greenberg. Thermochromic vanadium oxide with depressed switching temperature, US patent 4401690, 1983.
- [2] G. V. Jorgenson and J. C. Lee. Doped vanadium oxide for optical switching films. *Sol. Energy Mater.*, 14(3-5):205, 1986.
- [3] S. M. Babulanam, T. S. Eriksson, G. A. Niklasson, and C. G. Granqvist. Thermochromic VO<sub>2</sub> films for energy-efficient windows. *Sol. Energy Mater.*, 5(16):347, 1987.
- [4] F. J. Morin. Oxides which show a metal-to-insulator transition at the Neel temperature. *Phys. Rev. Lett.*, 3(1):34–36, Jul 1959.
- [5] C G Granqvist. Spectrally selective coatings for energy efficiency and solar applications. *Physica Scripta*, 32(4):401–407, 1985.
- [6] M. Imada, A. Fujimori, and Y. Tokura. Metal-insulator transitions. *Rev. Mod. Phys.*, 70(4):1039–1263, Oct 1998.
- [7] M. N. Baibich, J. M. Broto, A. Fert, F. Nguyen Van Dau, F. Petroff, P. Eitenne, G. Creuzet, A. Friederich, and J. Chazelas. Giant magnetoresistance of (001)Fe/(001)Cr magnetic superlattices. *Phys. Rev. Lett.*, 61(21):2472–2475, Nov 1988.
- [8] G. Binasch, P. Grünberg, F. Saurenbach, and W. Zinn. Enhanced magnetoresistance in layered magnetic structures with antiferromagnetic interlayer exchange. *Phys. Rev. B*, 39(7):4828–4830, Mar 1989.
- [9] Y. Paz, Z. Luo, L. Rabenberg, and A. Heller. Photooxidative self-cleaning transparent titanium dioxide films on glass. *J. Mater. Res.*, 10:2842, 1995.
- [10] L. Hedin. New method for calculating the one-particle Green's function with application to the electron-gas problem. *Phys. Rev.*, 139(3A):A796–A823, Aug 1965.

- [11] F Aryasetiawan and O Gunnarsson. The GW method. *Rep. Prog. Phys.*, 61(3):237–312, 1998.
- [12] M. van Schilfhaarde, Takao Kotani, and S. Faleev. Quasiparticle self-consistent GW theory. *Phys. Rev. Lett.*, 96(22):226402, 2006.
- [13] Fabien Bruneval, Nathalie Vast, and Lucia Reining. Effect of self-consistency on quasiparticles in solids. *Phys. Rev. B*, 74(4):045102, 2006.
- [14] Giovanni Onida, Lucia Reining, and Angel Rubio. Electronic excitations: Density-functional versus many-body Green’s-function approaches. *Rev. Mod. Phys.*, 74(2):601–659, Jun 2002.
- [15] R. O. Jones and O. Gunnarsson. The density functional formalism, its applications and prospects. *Rev. Mod. Phys.*, 61(3):689–746, Jul 1989.
- [16] A. Georges, G. Kotliar, W. Krauth, and M. J. Rozenberg. Dynamical mean-field theory of strongly correlated fermion systems and the limit of infinite dimensions. *Rev. Mod. Phys.*, 68(1):13, Jan 1996.
- [17] V I Anisimov, A I Poteryaev, M A Korotin, A O Anokhin, and G Kotliar. First-principles calculations of the electronic structure and spectra of strongly correlated systems: dynamical mean-field theory. *J. Phys.: Cond. Matter*, 9(35):7359–7367, 1997.
- [18] A. I. Lichtenstein and M. I. Katsnelson. Ab initio calculations of quasiparticle band structure in correlated systems: LDA++ approach. *Phys. Rev. B*, 57(12):6884–6895, Mar 1998.
- [19] G. Kotliar and D. Vollhardt. Strongly correlated materials: Insights from dynamical mean-field theory. *Physics Today*, 57(3):53, 2004.
- [20] K. Held, I. A. Nekrasov, G. Keller, V. Eyert, N. Blümer, A. K. McMahan, R. T. Scalettar, Th. Pruschke, V. I. Anisimov, and D. Vollhardt. Realistic investigations of correlated electron systems within LDA+DMFT. *Psi-k Newsletter*, 56(65), 2003.
- [21] S. Biermann. LDA+DMFT - a tool for investigating the electronic structure of materials with strong electronic coulomb correlations. *in Encyclopedia of Materials: Science and Technology*, 2006.
- [22] S. Biermann, A. Dallmeyer, C. Carbone, W. Eberhardt, C. Pampuch, O. Rader, M. I. Katsnelson, and A. I. Lichtenstein. Observation of Hubbard bands in gamma-manganese. *JETP Letters and condmat0112430*, 80(9):612, 2004.
- [23] S. Biermann. PhD thesis. University of Cologne, 2000.
- [24] A. I. Lichtenstein, M. I. Katsnelson, and G. Kotliar. Finite-temperature magnetism of transition metals: An ab initio dynamical mean-field theory. *Phys. Rev. Lett.*, 87:067205, 2001.
- [25] J. Braun, J. Minár, H. Ebert, M. I. Katsnelson, and A. I. Lichtenstein. Spectral function of ferromagnetic 3d metals: A self-consistent LSDA + DMFT approach combined with the one-step model of photoemission. *Physical Review Letters*, 97(22):227601, 2006.

- [26] I. A. Nekrasov, K. Held, G. Keller, D. E. Kondakov, Th. Pruschke, M. Kollar, O. K. Andersen, V. I. Anisimov, and D. Vollhardt. Momentum-resolved spectral functions of SrVO<sub>3</sub> calculated by LDA + DMFT. *Phys. Rev. B*, 73(15):155112, 2006.
- [27] K. Held, G. Keller, V. Eyert, D. Vollhardt, and V. I. Anisimov. Mott-Hubbard metal-insulator transition in paramagnetic V<sub>2</sub>O<sub>3</sub>: An LDA+DMFT (QMC) study. *Phys. Rev. Lett.*, 86(23):5345–5348, Jun 2001.
- [28] A. Liebsch. Surface versus bulk coulomb correlations in photoemission spectra of SrVO<sub>3</sub> and CaVO<sub>3</sub>. *Phys. Rev. Lett.*, 90(9):096401, Mar 2003.
- [29] E. Pavarini, S. Biermann, A. Poteryaev, A. I. Lichtenstein, A. Georges, and O. K. Andersen. Mott transition and suppression of orbital fluctuations in orthorhombic 3d<sup>1</sup> perovskites. *Phys. Rev. Lett.*, 92(17):176403, 2004.
- [30] M. S. Laad, L. Craco, and E. Müller-Hartmann. Orbital switching and the first-order insulator-metal transition in paramagnetic V<sub>2</sub>O<sub>3</sub>. *Phys. Rev. Lett.*, 91(15):156402, Oct 2003.
- [31] Alexander I. Poteryaev, Jan M. Tomczak, Silke Biermann, Antoine Georges, Alexander I. Lichtenstein, Alexey N. Rubtsov, Tanusri Saha-Dasgupta, and Ole K. Andersen. Enhanced crystal-field splitting and orbital-selective coherence induced by strong correlations in V<sub>2</sub>O<sub>3</sub>. *Phys. Rev. B*, 76(8):085127, 2007.
- [32] S. Biermann, A. Poteryaev, A. I. Lichtenstein, and A. Georges. Dynamical singlets and correlation-assisted peierls transition in VO<sub>2</sub>. *Phys. Rev. Lett.*, 94(2):026404, 2005.
- [33] J. M. Tomczak, F. Aryasetiawan, and S. Biermann. Effective bandstructure in the insulating phase versus strong dynamical correlations in metallic VO<sub>2</sub>. 2008. submitted to Phys. Rev. B, preprint: arXiv:0704.0902.
- [34] Jan M. Tomczak. *Spectral and Optical Properties of Correlated Materials*. PhD thesis, Ecole Polytechnique, France, 2007.
- [35] Frank Lechermann, Silke Biermann, and Antoine Georges. Importance of interorbital charge transfers for the metal-to-insulator transition of BaVS<sub>3</sub>. *Phys. Rev. Lett.*, 94(16):166402, Apr 2005.
- [36] Frank Lechermann, Silke Biermann, and Antoine Georges. Competing itinerant and localized states in strongly correlated BaVS<sub>3</sub>. *Phys. Rev. B*, 76(8):085101, 2007.
- [37] M. B. Zöfl, I. A. Nekrasov, Th. Pruschke, V. I. Anisimov, and J. Keller. Spectral and magnetic properties of  $\alpha$ - and  $\gamma$ -Ce from dynamical mean-field theory and local density approximation. *Phys. Rev. Lett.*, 87(27):276403, Dec 2001.
- [38] K. Held, A. K. McMahan, and R. T. Scalettar. Cerium volume collapse: Results from the merger of dynamical mean-field theory and local density approximation. *Phys. Rev. Lett.*, 87(27):276404, Dec 2001.

- [39] B. Amadon, S. Biermann, A. Georges, and F. Aryasetiawan. The alpha-gamma transition of cerium is entropy driven. *Physical Review Letters*, 96(6):066402, 2006.
- [40] S. Y. Savrasov, G. Kotliar, and E. Abrahams. Correlated electrons in  $\delta$ -plutonium within a dynamical mean-field picture. *Nature*, 410(6830):793, 2001.
- [41] G. Kotliar, S. Y. Savrasov, K. Haule, V. S. Oudovenko, O. Parcollet, and C. A. Marianetti. Electronic structure calculations with dynamical mean-field theory. *Rev. Mod. Phys.*, 78(3):865–951, Aug 2006.
- [42] A. J. Millis. Optical conductivity and correlated electron physics. In L. Degiorgi D. Baeriswyl, editor, *Strong Interactions in Low Dimensions*, volume 25, page 195ff. Physics and Chemistry of Materials with Low-Dimensional Structures, 2004.
- [43] M. Dressel and G. Grüner. *Electrodynamics of Solids*. Cambridge University Press, 2003.
- [44] Andrea Damascelli, Zahid Hussain, and Zhi-Xun Shen. Angle-resolved photoemission studies of the cuprate superconductors. *Rev. Mod. Phys.*, 75(2):473–541, Apr 2003.
- [45] Anil Khurana. Electrical conductivity in the infinite-dimensional Hubbard model. *Phys. Rev. Lett.*, 64(16):1990, Apr 1990.
- [46] M. J. Rozenberg, G. Kotliar, H. Kajueter, G. A. Thomas, D. H. Rapkine, J. M. Honig, and P. Metcalf. Optical conductivity in Mott-Hubbard systems. *Phys. Rev. Lett.*, 75(1):105–108, Jul 1995.
- [47] M. J. Rozenberg, G. Kotliar, and H. Kajueter. Transfer of spectral weight in spectroscopies of correlated electron systems. *Phys. Rev. B*, 54(12):8452–8468, Sep 1996.
- [48] Th. Pruschke, D. L. Cox, and M. Jarrell. Hubbard model at infinite dimensions: Thermodynamic and transport properties. *Phys. Rev. B*, 47(7):3553–3565, Feb 1993.
- [49] M. Jarrell, J. K. Freericks, and Th. Pruschke. Optical conductivity of the infinite-dimensional Hubbard model. *Phys. Rev. B*, 51(17):11704–11711, May 1995.
- [50] N. Blümer. *Mott-Hubbard Metal-Insulator Transition and Optical Conductivity in High Dimensions*. PhD thesis, Universität Augsburg, 2002.
- [51] N. Blümer and P. G. J. van Dongen. Transport properties of correlated electrons in high dimensions, 2003.
- [52] E Pavarini, A Yamasaki, J Nuss, and O K Andersen. How chemistry controls electron localization in  $3d^1$  perovskites: a Wannier-function study. *New Journal of Physics*, 7:188, 2005.
- [53] L. Baldassarre, A. Perucchi, D. Nicoletti, A. Toschi, G. Sangiovanni, K. Held, M. Capone, M. Ortolani, L. Malavasi, M. Marsi, P. Metcalf, P. Postorino, and S. Lupi. Quasiparticle evolution and pseudogap formation in  $V_2O_3$ : An infrared spectroscopy study. *Phys. Rev. B*, 77(11):113107, 2008.



- [54] G. Pálsson. *Computational studies of thermoelectricity in strongly correlated electron systems*. PhD thesis, Rutgers, The State University of New Jersey, 2001.
- [55] J. M. Tomczak and S. Biermann. Materials design using correlated oxides: Optical properties of vanadium dioxide. 2008. submitted to *Phys. Rev. Lett.*, preprint: arXiv:0807.4044.
- [56] J. M. Tomczak and S. Biermann. Optical properties of strongly correlated materials – generalized peierls approach and its application to VO<sub>2</sub>. 2008. in preparation.
- [57] J. M. Tomczak and S. Biermann. Multi-orbital effects in optical properties of vanadium sesquioxide. 2008. submitted to *J. Phys.: Cond. Matter*.
- [58] A. Perlov, S. Chadov, and H. Ebert. Green function approach for the ab initio calculation of the optical and magneto-optical properties of solids: Accounting for dynamical many-body effects. *Phys. Rev. B*, 68(24):245112, Dec 2003.
- [59] A. Perlov, S. Chadov, H. Ebert, L. Chioncel, A.I. Lichtenstein, and M.I. Katsnelson. Ab-initio calculations of the optical and magneto-optical properties of moderately correlated systems: accounting for correlation effects. *Physics of Spin in Solids: Materials, Methods & Applications, October 15-19, 2003, Baku, Azerbaijan*, 2004.
- [60] V. S. Oudovenko, G. Palsson, S. Y. Savrasov, K. Haule, and G. Kotliar. Calculations of optical properties in strongly correlated materials. *Phys. Rev. B*, 70(12):125112, 2004.
- [61] Kristjan Haule, Viktor Oudovenko, Sergej Y. Savrasov, and Gabriel Kotliar. The alpha → gamma transition in Ce: A theoretical view from optical spectroscopy. *Phys. Rev. Lett.*, 94(3):036401, 2005.
- [62] J. H. Shim, K. Haule, and G. Kotliar. Modeling the localized-to-itinerant electronic transition in the heavy fermion system CeIrIn<sub>5</sub>. *Science*, 318(5856):1615–1617, 2007.
- [63] F. Lechermann, A. Georges, A. Poteryaev, S. Biermann, M. Posternak, A. Yamasaki, and O. K. Andersen. Dynamical mean-field theory using wannier functions: A flexible route to electronic structure calculations of strongly correlated materials. *Phys. Rev. B*, 74(12):125120, 2006.
- [64] V. Eyert. The metal-insulator transitions of VO<sub>2</sub>: A band theoretical approach. *Ann. Phys. (Leipzig)*, 11:650, 2002.
- [65] R. M. Wentzcovitch, W. W. Schulz, and P. B. Allen. VO<sub>2</sub>: Peierls or Mott-Hubbard? A view from band theory. *Phys. Rev. Lett.*, 72(21):3389–3392, May 1994.
- [66] M. S. Laad, L. Craco, and E. Müller-Hartmann. VO<sub>2</sub>: A two-fluid incoherent metal? *Europhys. Lett.*, 69(6):984–989, 2005.
- [67] A. Liebsch, H. Ishida, and G. Bihlmayer. Coulomb correlations and orbital polarization in the metal-insulator transition of VO<sub>2</sub>. *Phys. Rev. B*, 71(8):085109, 2005.
- [68] T. C. Koethe, Z. Hu, M. W. Haverkort, C. Schussler-Langeheine, F. Venturini, N. B. Brookes, O. Tjernberg, W. Reichelt, H. H. Hsieh, H.-J. Lin, C. T. Chen, and L. H. Tjeng.

- Transfer of spectral weight and symmetry across the metal-insulator transition in VO<sub>2</sub>. *Phys. Rev. Lett.*, 97(11):116402, 2006.
- [69] A. Continenza, S. Massidda, and M. Posternak. Self-energy corrections in VO<sub>2</sub> within a model GW scheme. *Phys. Rev. B*, 60(23):15699–15704, Dec 1999.
- [70] Matteo Gatti, Fabien Bruneval, Valerio Olevano, and Lucia Reining. Understanding correlations in vanadium dioxide from first principles. *Phys. Rev. Lett.*, 99(26):266402, 2007.
- [71] R. Sakuma, T. Miyake, and F. Aryasetiawan. First-principles study of correlation effects in VO<sub>2</sub>: Peierls vs. Mott-Hubbard. 2008.
- [72] J. M. Tomczak and S. Biermann. Effective band structure of correlated materials: The case of VO<sub>2</sub>. *J. Phys.: Cond. Matter*, 19(36):365206, 2007.
- [73] Hans W. Verleur, A. S. Barker, and C. N. Berglund. Optical properties of VO<sub>2</sub> between 0.25 and 5 eV. *Phys. Rev.*, 172(3):788–798, Aug 1968.
- [74] M. M. Qazilbash, K. S. Burch, D. Whisler, D. Shrekenhamer, B. G. Chae, H. T. Kim, and D. N. Basov. Correlated metallic state of vanadium dioxide. *Phys. Rev. B*, 74(20):205118, 2006.
- [75] K. Okazaki, S. Sugai, Y. Muraoka, and Z. Hiroi. Role of electron-electron and electron-phonon interaction effects in the optical conductivity of VO<sub>2</sub>. *Phys. Rev. B*, 73(16):165116, Apr 2006.
- [76] M. M. Qazilbash, M. Brehm, Byung-Gyu Chae, P.-C. Ho, G. O. Andreev, Bong-Jun Kim, Sun Jin Yun, A. V. Balatsky, M. B. Maple, F. Keilmann, Hyun-Tak Kim, and D. N. Basov. Mott transition in VO<sub>2</sub> revealed by infrared spectroscopy and nano-imaging. *Science*, 318(5857):1750–1753, 2007.
- [77] J. B. Goodenough. The two components of the crystallographic transition in VO<sub>2</sub>. *J. Solid State Chem.*, 3:490–500, Mar 1971.
- [78] C. G. Granqvist. Window coatings for the future. *Thin Solid Films*, 193-194(Part 2):730–741, Dec 1990.
- [79] Elizabeth E. Chain. Optical properties of vanadium dioxide and vanadium pentoxide thin films. *Appl. Opt.*, 30(19):2782, 1991.
- [80] C. G. Granqvist. Transparent conductors as solar energy materials: A panoramic review. *Solar Energy Materials and Solar Cells*, 91(17):1529, Oct 2007.
- [81] M. A. Sobhan, R. T. Kivaisi, B. Stjerna, and C. G. Granqvist. Thermo-chromism of sputter deposited W<sub>x</sub>V<sub>1-x</sub>O<sub>2</sub> films, solar energy materials and solar cells. *Sol. Energy Mater. Sol. Cells*, 44(4):451, 1996.
- [82] W. Burkhardt, T. Christman, S. Franke, W. Kriegseis, D. Meister, B. K. Meyer, W. Niessner, D. Schalch, and A. Scharmann. Tungsten and fluorine co-doping of VO<sub>2</sub> films. *Thin Solis Films*, 402(1-2):226, Jan 2002.

- [83] W. Burkhardt, T. Christmann, B. K. Meyer, W. Niessner, D. Schalch, and A. Scharmann. W- and F-doped VO<sub>2</sub> films studied by photoelectron spectrometry. *Thin Solis Films*, 345(2):229, May 1999.
- [84] P. Jin, G. Xu, M. Tazawa, and K. Yoshimura. Design, formation and characterization of a novel multifunctional window with VO<sub>2</sub> and TiO<sub>2</sub> coatings. *Appl. Phys. A*, 77:455, 2003.
- [85] M. Born and E. Wolf. *Principles of optics: electromagnetic theory of propagation, interference and diffraction of light*. Oxford, Pergamon Press, 1964.
- [86] Masato Tazawa, Ping Jin, and Sakae Tanemura. Optical constants of V<sub>1-x</sub>W<sub>x</sub>O<sub>2</sub> films. *Appl. Opt.*, 37(10):1858–1861, 1998.
- [87] S. Biermann, F. Aryasetiawan, and A. Georges. First-principles approach to the electronic structure of strongly correlated systems: Combining the GW approximation and dynamical mean-field theory. *Phys. Rev. Lett.*, 90(8):086402, Feb 2003.
- [88] V. I. Anisimov and O. Gunnarsson. Density-functional calculation of effective coulomb interactions in metals. *Phys. Rev. B*, 43(10):7570–7574, Apr 1991.
- [89] F. Aryasetiawan, M. Imada, A. Georges, G. Kotliar, S. Biermann, and A. I. Lichtenstein. Frequency-dependent local interactions and low-energy effective models from electronic structure calculations. *Phys. Rev. B*, 70(19):195104, Nov 2004.
- [90] T. Miyake and F. Aryasetiawan. Screened coulomb interaction in the maximally localized Wannier basis. *Phys. Rev. B*, 77:085122, 2008.
- [91] F. Aryasetiawan, S. Biermann, and A. Georges. A first principles scheme for calculating the electronic structure of strongly correlated materials: GW+DMFT. *Proceedings of the conference "Coincidence Studies of Surfaces, Thin Films and Nanostructures"*, Ringberg castle, Sept. 2003, 2004.
- [92] S. Biermann, F. Aryasetiawan, and A. Georges. Electronic structure of strongly correlated materials: towards a first principles scheme. *Proceedings of the NATO Advanced Research Workshop on "Physics of Spin in Solids: Materials, Methods, and Applications" in Baku, Azerbaijan, Oct. 2003. NATO Science Series II, Kluwer Academic Publishers B.V*, 2004.
- [93] K. Nakamura, R. Arita, and M. Imada. Ab initio derivation of low-energy model for iron-based superconductors LaFeAsO and LaFePO. 2008. arXiv:0806.4750.
- [94] V. I. Anisimov, Dm M. Korotin, S. V. Streltsov, A. V. Kozhevnikov, J. Kunes, A. O. Shorikov, and M. A. Korotin. Coulomb parameter U and correlation strength in LaFeAsO. 2008. arXiv:0807.0547.